

# Monitoring statistics of the ERS-2 scatterometer for ESA

## cycle 87

(Project Ref. 15988/02/I-LG)

Hans Hersbach  
European Centre for Medium-Range Weather Forecasts,  
Shinfield Park, Reading, RG2 9AX, England  
Tel: (+44 118) 9499476, e-mail: dal@ecmwf.int

September 22, 2003

## 1 Introduction

From 12 December 2001 onwards, ESRIN has redistributed ERS-2 scatterometer data to a selected group of users. On 4 February 2003, a new processor, ESACA, was introduced. It is an upgrade of the existing LRDPF and includes new scatterometer processing algorithms that anticipate errors in the satellites yaw attitude control. It was installed for Kiruna station only.

On 22 June 2003, both LBR tape recorders failed, with the consequence that after that event data is only retained for regions for which the satellite has direct visual contact with a ground station. For Kiruna station this means restriction to the North Atlantic.

On 21 August 2003, the world-wide dissemination of ERS-2 data was restarted. At ECMWF, the first data was received for 15:50 UTC that day. Since that date, data from other ground stations (Maspalomas, Gatineau, and Frascati) has been received as well, resulting in a much wider coverage. For cycle 87, most of the North-Atlantic was covered, part of the Mediterranean, the Gulf of Mexico, and a small part of the Pacific north-west from the US and Canada.

The quality of the new UWI product was monitored at ECMWF for cycle 87. Results were compared to those obtained from the previous cycle, as well for data received during the nominal period in 2000 (up to cycle 59).

The scatterometer data was not used in the 4D-Var data assimilation system at ECMWF. However, it is being processed passively, with the aim that it will become active within the next few months.

During cycle 87, data was received between 09:06 UTC 11 August and 19:31 UTC 15 September 2003. From 15:50 UTC 21 August 2003 onwards, this was the new world-wide distributed UWI data. Before that date, data was received from Kiruna station only, which led to low or zero data volumes for 6-hourly batches centered around 00 UTC. After the re-introduction of 15 September, data volumes became more evenly distributed in time. No data was received for the two 6-hourly batches of 18 UTC 24 August and 00 UTC 25 August 2003.

Time series for the asymmetry between the incidence angles of the fore and aft beam (related to yaw attitude errors) show several peaks, with amplitudes up to 3.0 degrees. No clear signals for enhanced solar activity were observed.

The re-disseminated UWI data are based on a new BUFR encoder for the ESACA processor. The issue on  $k_p$  scaling, as reported in cycle 81, has been resolved, with the result that the original quality control on its value exceeding the 10% level could be resumed in the monitoring. The content of the Missing Packet Counter has changed, low values now being better than high values. The QC on this quantity, therefore, was not resumed. Besides the encoding, the ESACA processor was updated as well. The discrepancy between UWI winds and CMOD4 winds, the latter being of considerably higher quality, has been resolved. This was confirmed by the monitoring at ECMWF.

Part of the improved quality of the UWI product is masked by the difference in data coverage. For instance, the standard deviation of de-aliases CMOD4 winds as compared to ECMWF first-guess winds (FGAT) has increased somewhat, which partly, must be the result of the more extreme wind climate in the larger area for cycle 87. The number of collocations of low UWI winds with high FGAT winds is comparable to that for the previous cycle.

Compared to nominal data in 2000, bias levels compared to FGAT winds were found to be very similar, both in sigma0 space as in wind domain. Even internode and inter-beam dependencies were found to be almost identical to the old situation. Standard deviations of wind speed, are lower than for 2000. Here the difference in coverage (North-Atlantic versus global) makes a direct comparison difficult. The inter-beam dependency of standard deviation may be expected to depend less on the area under consideration. It was found that UWI winds compare best to FGAT winds for the highest nodes, while this used to be around node 5, and being worse in the far range.

Although performing much better than for the nominal period in 2000, the de-aliasing algorithm of the revised ESACA processor seems to be less optimal than for its original version.

The ECMWF assimilation system was not changed during cycle 87.

## 2 ERS-2 statistics from 12 August to 15 September 2003

### 2.1 Sigma0 bias levels

The average sigma0 bias levels (compared to simulated sigma0's based on ECMWF model first-guess winds) stratified with respect to antenna beam, ascending or descending track and as function of incidence angle (i.e. across-node number) is displayed in Figure 1.

Compared to cycle 86, bias levels have become less negative. The situation is very similar to that of the nominal data in 2000 (see Figure 1 of the cyclic reports for cycle 48 to 59). The dependency of the bias as function of incidence angle is small, with a tendency of being somewhat more negative at the far range. Internode differences are small, with the bias of the far-range mid beam being slightly less negative. Bias levels are in between -0.35 and -1.0 dB.

The data volume of ascending tracks is one-third lower than that of descending tracks.

### 2.2 Incidence angles

For ESACA, across-node binning is, like the old processor, retained on a 25km mesh. From simple geometrical arguments it follows that variations in yaw attitude will lead to asymmetries between the incidence angles of the fore and aft beam. Indeed, this has been observed. Figure 2 gives a time evolution of this asymmetry, showing rapid variations, which are typical for yaw attitude errors. Peaks are similar to those observed during cycle 86.

### 2.3 Distance to cone history

The distance to the cone history is shown in Figure 3. Many peaks are due to low data volumes. For the remaining 6-hourly cycles data volumes are much lower than before as well. This makes it very difficult to identify peaks in the cone history with instrument anomalies, since statistical fluctuations are too large. The same picture emerged even more for data in cycle 86. In future it may be necessary to average data over longer periods, e.g., over 24 hours.

Compared to cycles before 86, the average cone distance is, like for cycle 86 higher. Especially at lower nodes the level is far above unity. The reason for this non-ideal situation is under investigation. Compared to cycle 86, the situation has slightly improved, though. Averaged over all nodes (see top panel of Figure 8), the level has decreased from 1.35 (cycle 86) to 1.30.

Note that after the re-dissemination on 21 August, in the far range the fraction of rejected observations has been drastically reduced. It is the result of the QC on  $k_p$  which is incorrect for the old BUFR encoding, and corrected for the new one (see the report for cycle 82 for details).

	cycle 86		cycle 87	
	UWI	CMOD4	UWI	CMOD4
speed STDV	1.45	1.37	1.43	1.42
node 1-2	1.42	1.43	1.47	1.45
node 3-4	1.37	1.36	1.44	1.43
node 5-7	1.38	1.31	1.40	1.40
node 8-10	1.39	1.27	1.42	1.41
node 11-14	1.44	1.31	1.40	1.39
node 15-19	1.50	1.38	1.39	1.39
speed BIAS	-0.96	-0.97	-0.75	-0.74
node 1-2	-1.54	-1.58	-1.17	-1.14
node 3-4	-1.25	-1.25	-0.96	-0.92
node 5-7	-0.98	-0.96	-0.77	-0.74
node 8-10	-0.74	-0.75	-0.62	-0.62
node 11-14	-0.70	-0.73	-0.59	-0.59
node 15-19	-0.79	-0.82	-0.60	-0.61
direction STDV	25.3	18.5	27.7	19.7
direction BIAS	-3.7	-4.3	-3.5	-3.6

Table 1: Biases and standard deviation of ERS-2 versus ECMWF FGAT winds in m/s for speed and degrees for direction

## 2.4 UWI minus First-Guess wind history

In Figure 4, the UWI minus ECMWF first-guess wind-speed history is plotted.

Like it is the case for the history of the cone distance, the low data volumes make it difficult to separate instrument anomalies from numerical noise. Averages over periods longer than 6 hours may be necessary in future.

Average bias levels and standard deviations of UWI winds relative to FGAT winds are displayed in Table 1. Due to the difference in data coverage, results for cycles 86 and 87 are to be compared with care. It is seen that the bias of both the UWI and CMOD4 product have been reduced by more than 0.2 m/s. The average bias level is close to that for the nominal data in 2000 (UWI: -0.75 m/s now, was -0.79 m/s for cycle 59).

For the first time since the introduction of the ESACA processor, the standard deviations for UWI and CMOD4 data are almost equal again. This, together with a scatterplot between both products (not shown) confirms that the deviation of the UWI product from CMOD4 inverted winds has been resolved (see also second panel of Figure 8). The enhancement of standard deviation of CMOD4 winds compared to cycle 86 (1.42 m/s, was 1.37 m/s) must for a part be the result of the difference in data coverage. Note that the present standard deviation of the UWI winds is well below that for nominal data in 2000 (1.43 m/s, was 1.57 m/s for cycle 59). Again, the large difference in coverage inhibits an exact comparison.

Internode differences in bias levels have been reduced substantially (see third panel of figure 8). Their present values are, again, very similar to the situation in

2000 (-1.17 m/s for node 1-2 to -0.60 for node 15-19; was -1.15 m/s respectively -0.62 for cycle 58). This is also illustrated in Figures 9 (top-middle panel) and 10 (top right panel), which show node-wise statistics for cycle 87 respectively the month December for the years 1997 to 2000. Both the bias levels for CMOD4 (dotted) and CMOD5 (solid) as function of node number are very similar to the situation for 2000.

The internode dependency of standard deviation, however, is different from the situation in 2000 (top right panel of Figure 9 and middle-right panel of Figure 10). Optimal results used to be achieved around node 5, and being worse in the far range. The situation is now more evenly distributed.

In the left panels of Figure 9, the number of observations are plotted (for wind direction winds only stronger than 4 m/s). From this it is seen that the volume in the far range is much lower than that in the near range. It appears that in the far range information on the fore or aft incidence angle is missing more often. This may be the reason for the above discussed change of the internode dependency of the standard deviation.

For cycle 87 the (scatterometer - model) direction standard deviations were ranging between 20 and 40 degrees (Figure 5). Sharp peaks are the result of low data volumes. For de-aliased CMOD4 winds values between 20 and 30 degrees are most common. On average (see Table 1), the quality of the UWI wind direction is lower than for cycle 86 (27.7 degrees, was 25.3 degrees, see also lower panel of Figure 8). It is the result of a jump in performance after the world-wide re-introduction of the UWI data on 21 August 2003. The quality of the de-aliased CMOD4 wind direction is lower as well (19.7 degrees versus 18.2 respectively 18.6 degrees). However, it does not show the jump at 21 August 2003. As a result it seems that the de-aliasing algorithm has become less optimal for the revised ESACA processor.

Node-wise averages for wind-direction performance are shown in the lower right panel of Figure 9. It shows that the quality of wind direction is best at high incidence angles. Values for de-aliased winds are very similar to those in 2000 (not shown).

In the top panel of Figure 10 all locations are plotted for which UWI winds were more than 6 m/s weaker than the FGAT winds (rather than 8 m/s, as plotted for previous cycles). There are no clear signs for instrument anomalies (such as occurred for cycle 83, and for cycles before the introduction of the ESACA processor), in which case large parts of tracks would appear in Figure 10.

For one case, wind fields are shown in the lower panel of Figure 10. It concerns data for hurricane Fabian, which was observed on 15 UTC 5 September 2003. Although the de-aliasing software resulted in the wrong solution in a patch of winds near its center, the flow of the UWI winds, being in detail different from that of the ECMWF analysis, looks realistic.

## 2.5 Scatter plots

Scatterplots of model 10 m first-guess winds versus ERS-2 winds are displayed in Figures 12 to 15. Values of standard deviations and biases are slightly different from those displayed in Table 1. Reason for this is that, for plotting purposes, the in 0.5 m/s resolution ERS-2 winds have been slightly perturbed (increases scatter with

0.02 m/s), and that zero wind-speed ERS-2 winds have been excluded (decreases scatter with about 0.05 m/s). These scatterplots elucidate trends described in the previous subsection.

The scatterplot of UWI wind speed versus FGAT (Figure 12) is very similar to that for (at ECMWF inverted) de-aliased CMOD4 winds (Figure 14). It confirms that the new version of ESACA has been updated correctly. The standard deviation for the CMOD4 winds is higher than for cycle 86 (1.44, m/s was 1.39 m/s). However, the wind climate is more extreme for the larger area covered during cycle 87. The wind bias has been reduced (-0.74 m/s, was -0.96 m/s).

The average bias of the UWI wind direction has hardly changed (Figure 13, -3.6 degrees, was -3.9 degrees).

Winds derived on the basis of CMOD5 are displayed in Figure 14. Compared to cycle 87, the bias level has become far less negative (-0.30 m/s, was -0.72 m/s). A detailed node-wise dependency is displayed in Figure 9 (solid lines). The wind speed bias is almost identical to that encountered in 2000 (see top left panel of Figure 10). The worse performance of CMOD5 for wind direction at lower nodes is to be investigated.

## Figure Captions

**Figure 1:** Ratio of  $\langle \sigma_0^{0.625} \rangle / \langle \text{CMOD4}(\text{FirstGuess})^{0.625} \rangle$  converted in dB for the fore beam (solid line), mid beam (dashed line) and aft beam (dotted line), as a function of incidence angle for descending and ascending tracks. The thin lines indicate the error bars on the estimated mean. First-guess winds are based on the in time closest (+3h, +6h, +9h, or +12h) T511 forecast field, and are bilinearly interpolated in space.

**Figure 2:** Time series of the difference in incidence angle between the fore and aft beam.

**Figure 3:** Mean normalized distance to the cone computed every 6 hours for nodes 1-2, 3-4, 5-7, 8-10, 11-14 and 15-19 (solid curve close to 1 when no instrumental problems are present). The dotted curve shows the number of incoming triplets in logarithmic scale (1 corresponds to 60,000 triplets) and the dashed one indicates the fraction of complete sea-located triplets rejected by ESA flags, or by the wind inversion algorithm (0: all data kept, 1: no data kept).

**Figure 4:** Mean (solid line) and standard deviation (dashed line) of the wind speed difference UWI - first guess for the data retained by the quality control.

**Figure 5:** Same as Fig. 4, but for the wind direction difference. Statistics are computed only for wind speeds higher than 4 m/s.

**Figures 6 and 7:** Same as Fig. 5 and 6 respectively, but for the de-aliased CMOD4 data.

**Figure 8:** Evolution of the performance of the ERS-2 scatterometer averaged over 5-weekly cycles from 12 December 2001 (cycle 69) to 15 September 2003 (end cycle 87) for the UWI product (solid, star) and de-aliased winds based on CMOD4 (dashed, diamond). For cycle 86 two values are plotted; the first value for the global set, the second one for the regional set. Dotted lines represent values for cycle 59 (5 December 2000 to 17 January 2001), i.e. the last stable cycle of the nominal period. From top to bottom panel are shown the normalized distance to the cone (CMOD4 only) the standard deviation of the wind speed compared to FGAT winds, the corresponding bias (for UWI winds the extreme inter-node averages are shown as well), and the standard deviation of wind direction compared to FGAT.

**Figure 9:** Node-wise averages of number of observations, bias and standard deviation for scatterometer winds versus ECMWF First-Guess winds for wind speed (top panels) and wind direction (lower panels, winds stronger than 4 m/s only) for cycle 87. Dashed curves are for the UWI product, dotted for the de-aliased CMOD4 and solid for the de-aliased CMOD5 winds.

**Figure 10:** Node-wise averages of bias, standard deviation and scatter index for scatterometer wind speeds versus ECMWF First-Guess wind speeds, for the month December in 1997, 1998, 1999 and 2000. Dotted curves are for de-aliased CMOD4 winds, dashed for the at KNMI developed prototype CMOD5 winds, and solid curves for CMOD5.

**Figure 11:** Top panel: locations of data during cycle 87 for which UWI winds (top panel), respectively CMOD5 winds (lower panel) are more than 6 m/s weaker than the collocated FGAT winds. Lower panel: UWI wind vectors (red) and collocated FGAT wind vectors (blue) for Hurricane Fabian, observed on 5 September 2003.

**Figure 12:** Two-dimensional histogram of first guess and UWI wind speeds, for the data kept by the quality control, including the QC on  $k_p$ . Circles denote the mean values in the y-direction, and squares those in the x-direction.

**Figure 13:** Same as Fig. 11, but for wind direction. Only wind speeds higher than 4m/s are taken into account.

**Figure 14:** Same as Fig. 11, but for de-aliased CMOD4 winds.

**Figure 15:** Same as Fig. 11, but for de-aliased CMOD5 winds.

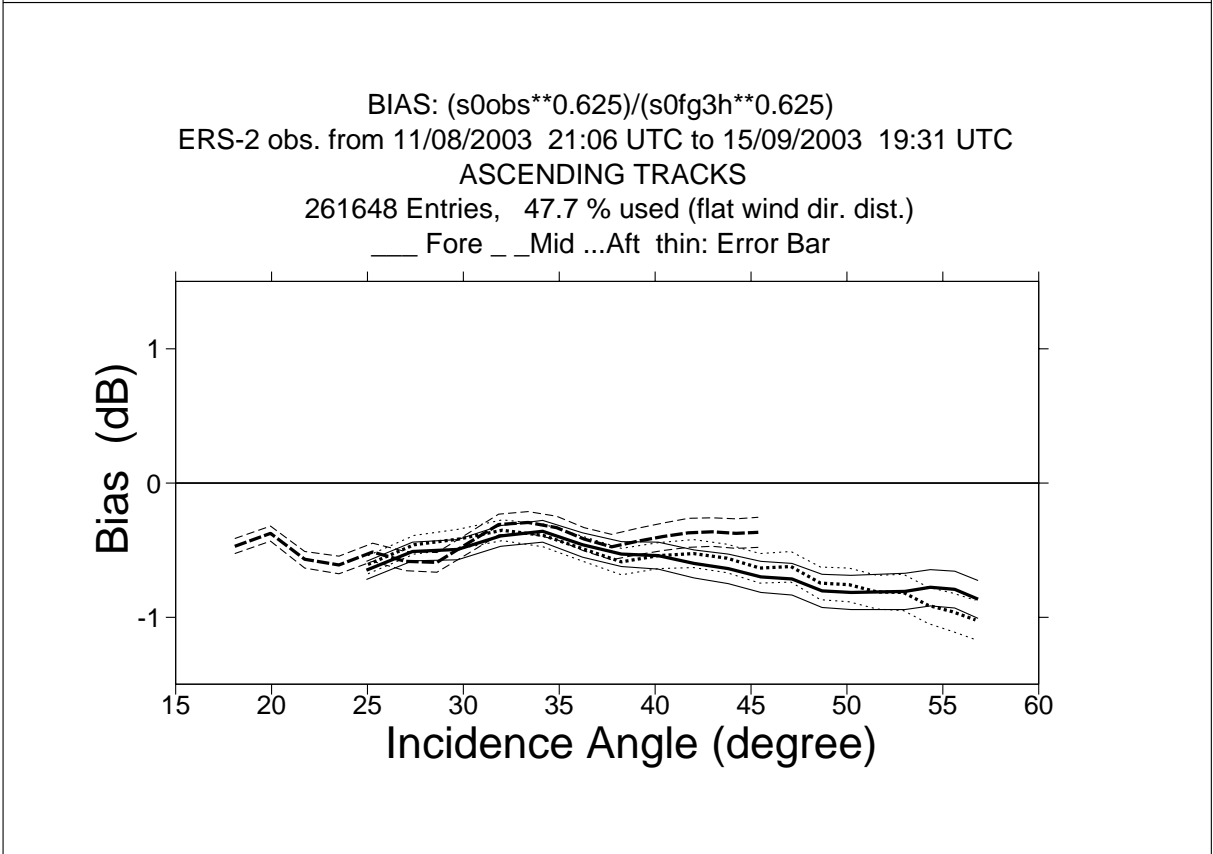
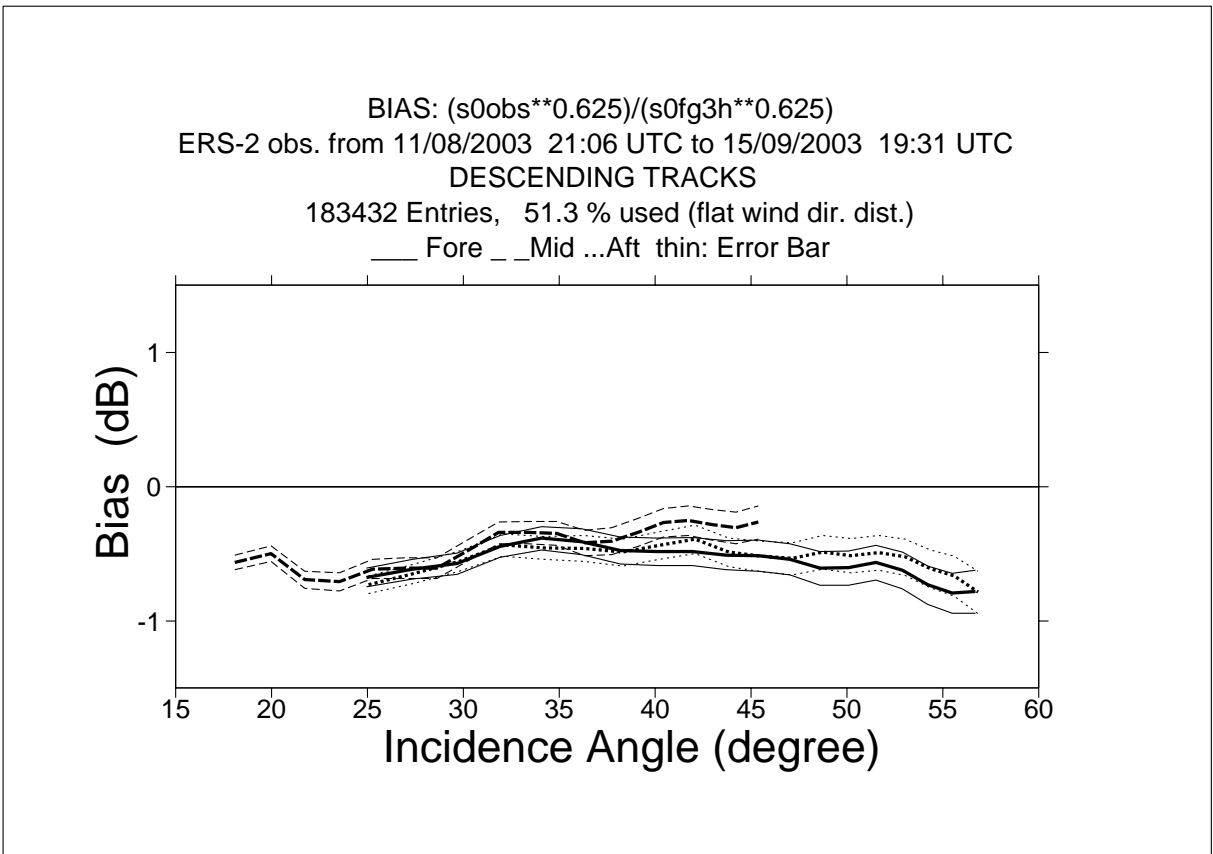


Figure 1

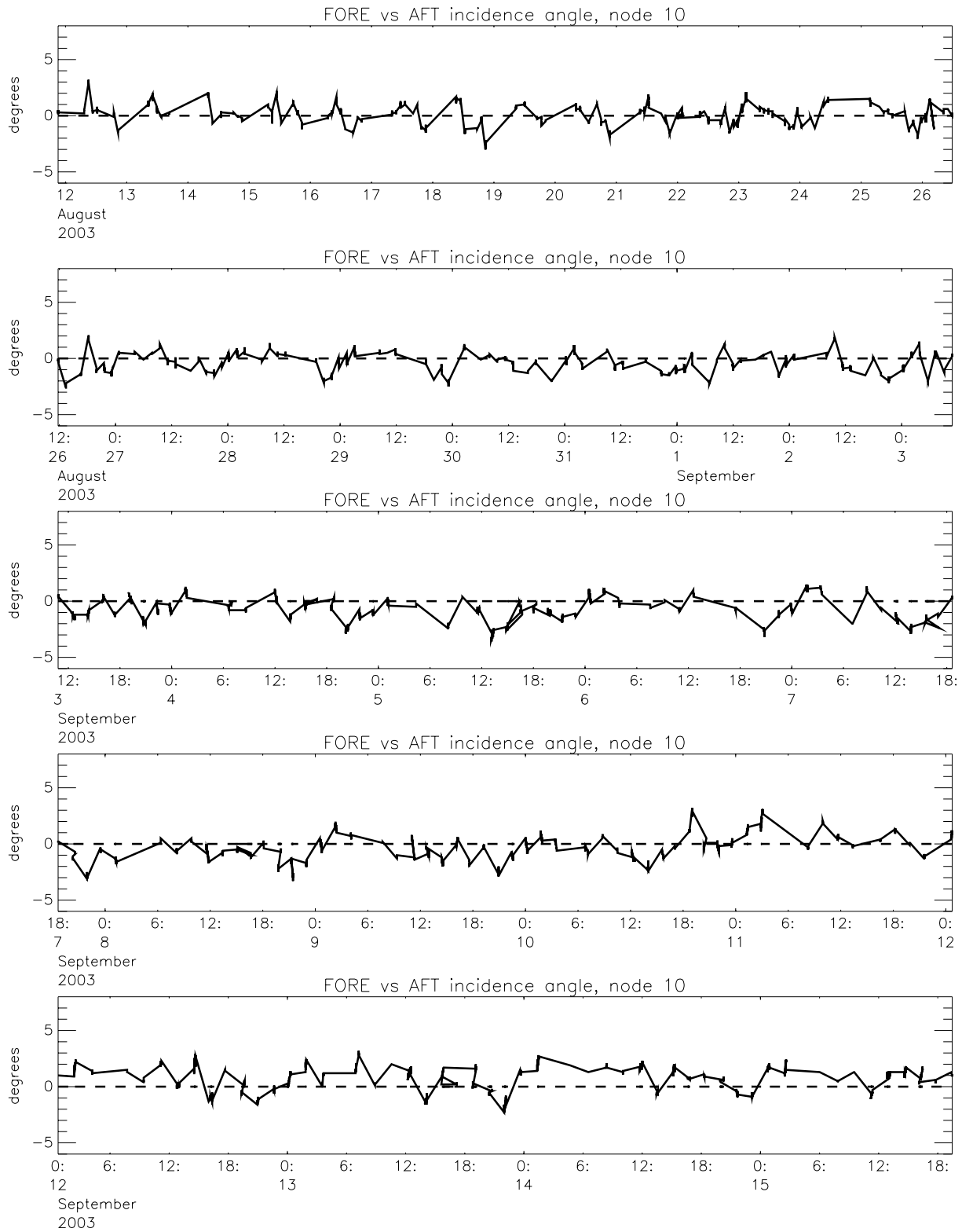


Figure 2

### Monitoring of Sigma0 triplets versus CMOD4 for ERS-2

from 2003081200 to 2003091518

(solid) mean normalised distance to the cone over 6 h

(dashed) fraction of complete sea-point observations rejected by ESA flag or CMOD4 inversion

(dotted) total number of data in log. scale (1 for 60000)

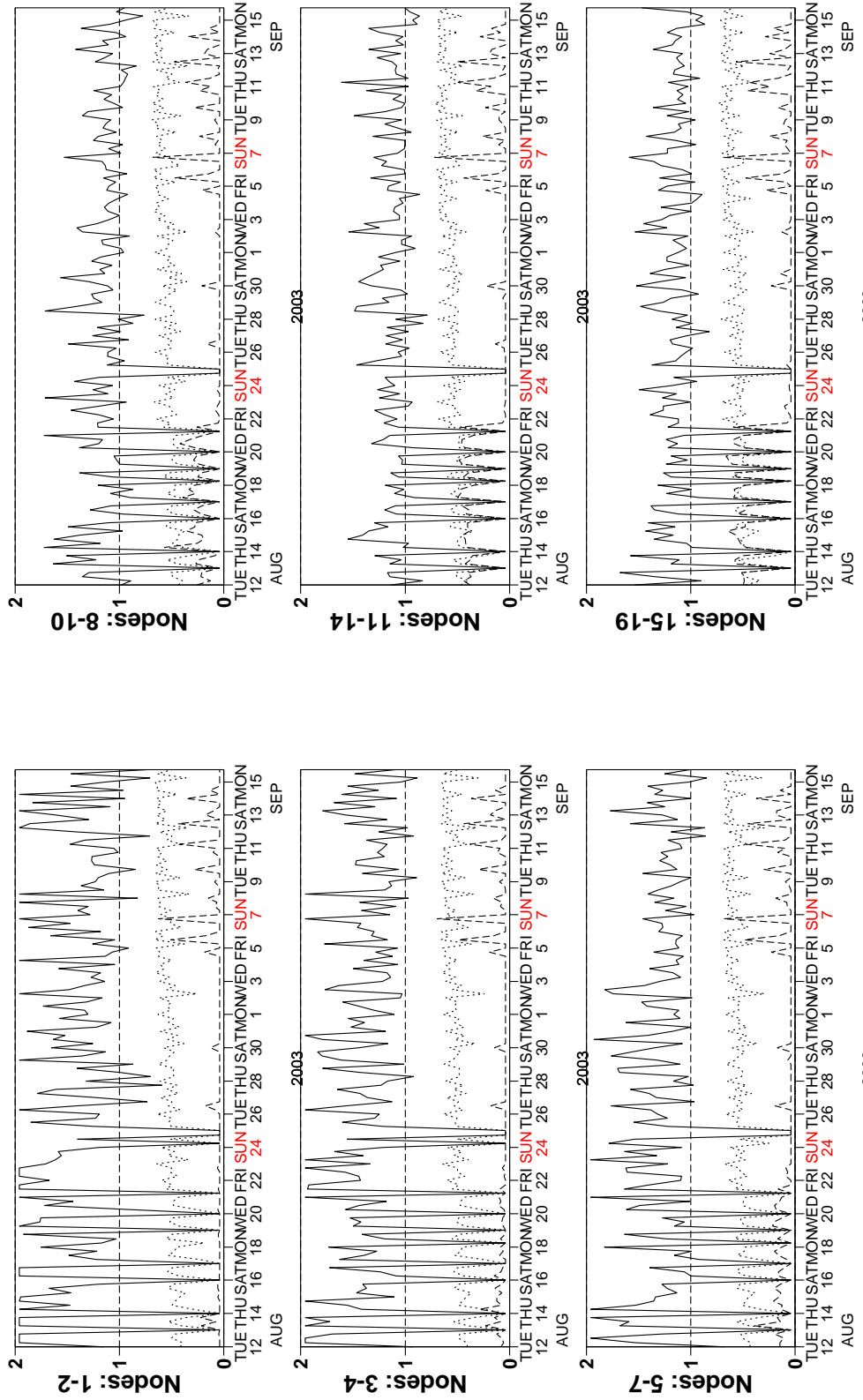


Figure 3

# Monitoring of UWI winds versus First Guess for ERS-2

from 2003081200 to 2003091518

(solid) wind speed bias UWI - First Guess over 6h (deg.)

(dashed) wind speed standard deviation UWI - First Guess over 6h (deg.)

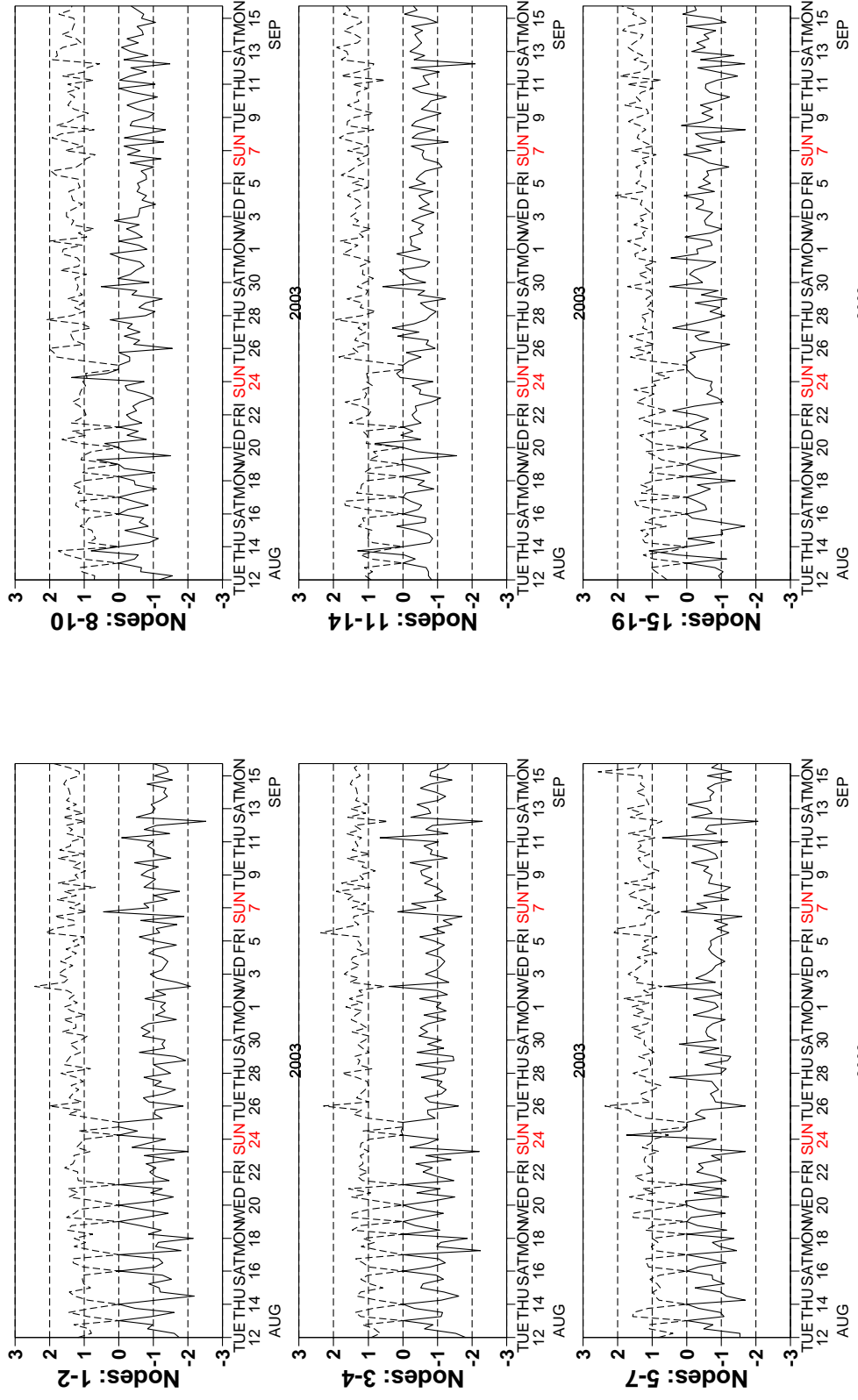


Figure 4

## Monitoring of UWI winds versus First Guess for ERS-2

from 2003081200 to 2003091518

(solid) wind direction bias UWI - First Guess over 6h (deg.)

(dashed) wind direction standard deviation UWI - First Guess over 6h (deg.)

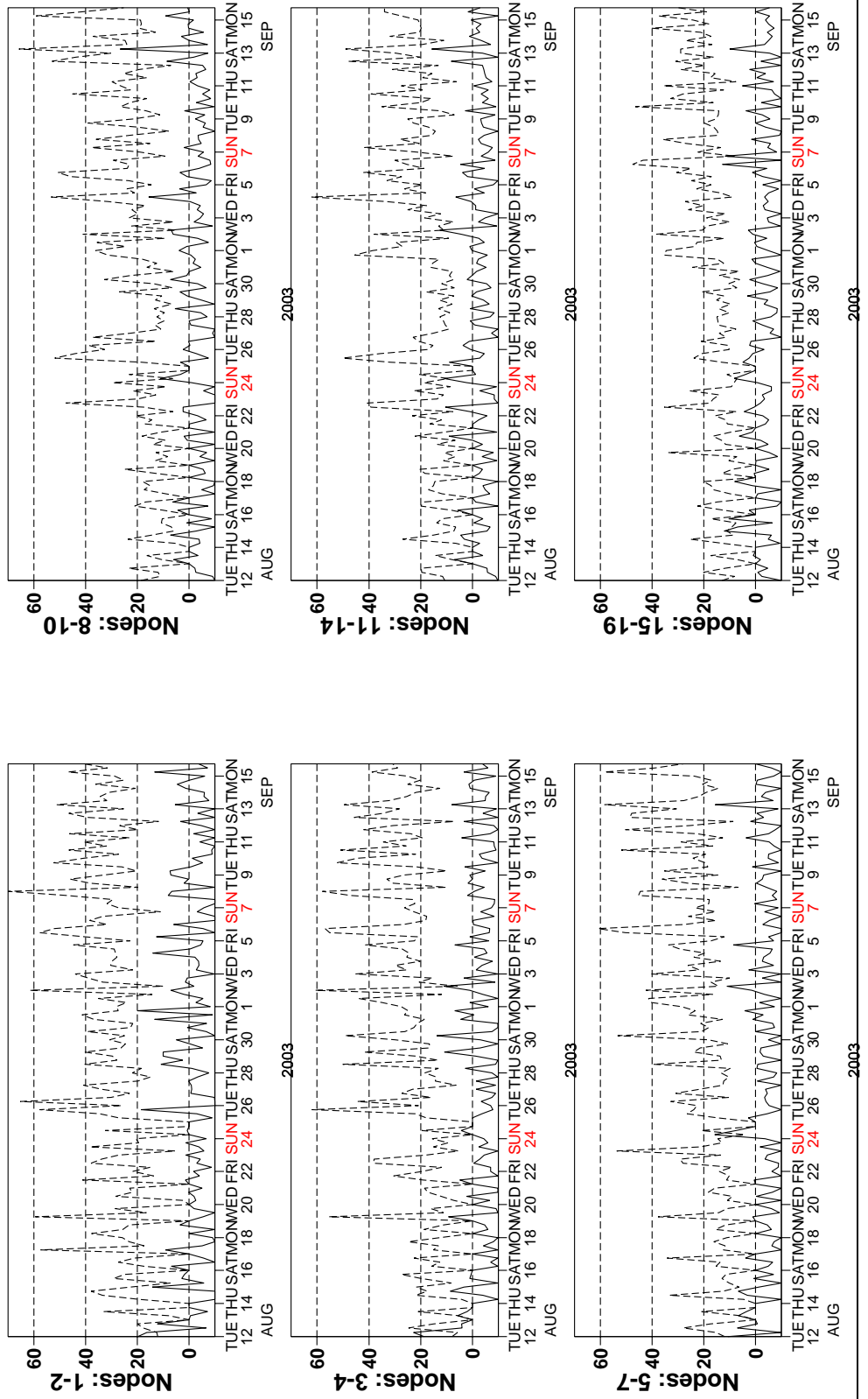


Figure 5

## Monitoring of de-aliased CMOD4 winds versus First Guess for ERS-2

from 2003081200 to 2003091518

(solid) wind speed bias CMOD4 - First Guess over 6h (deg.)

(dashed) wind speed standard deviation CMOD4 - First Guess over 6h (deg.)

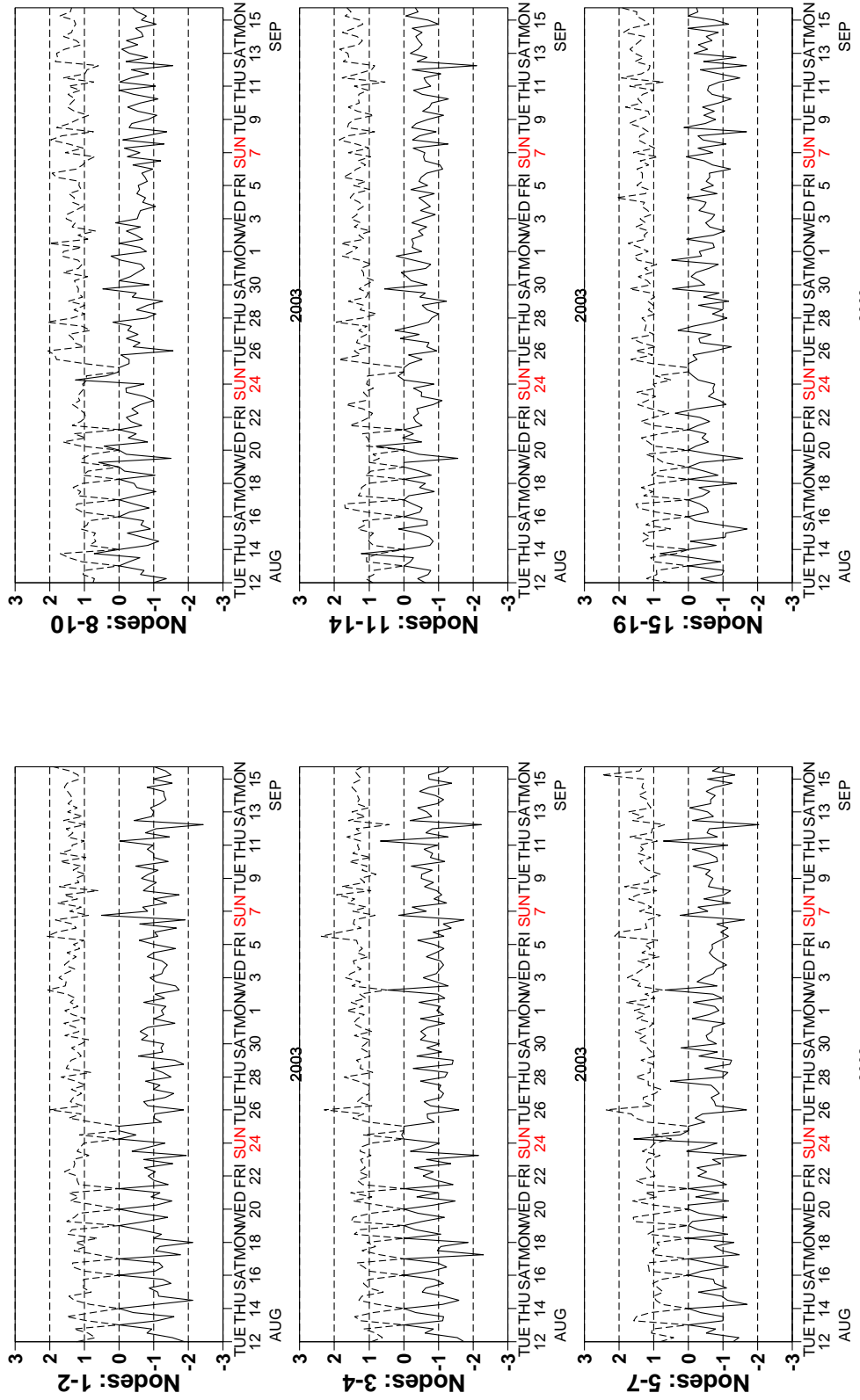


Figure 6

# Monitoring of de-aliased CMOD4 winds versus First Guess for ERS-2

from 2003081200 to 2003091518

(solid) wind direction bias CMOD4 - First Guess over 6h (deg.)

(dashed) wind direction standard deviation CMOD4 - First Guess over 6h (deg.)

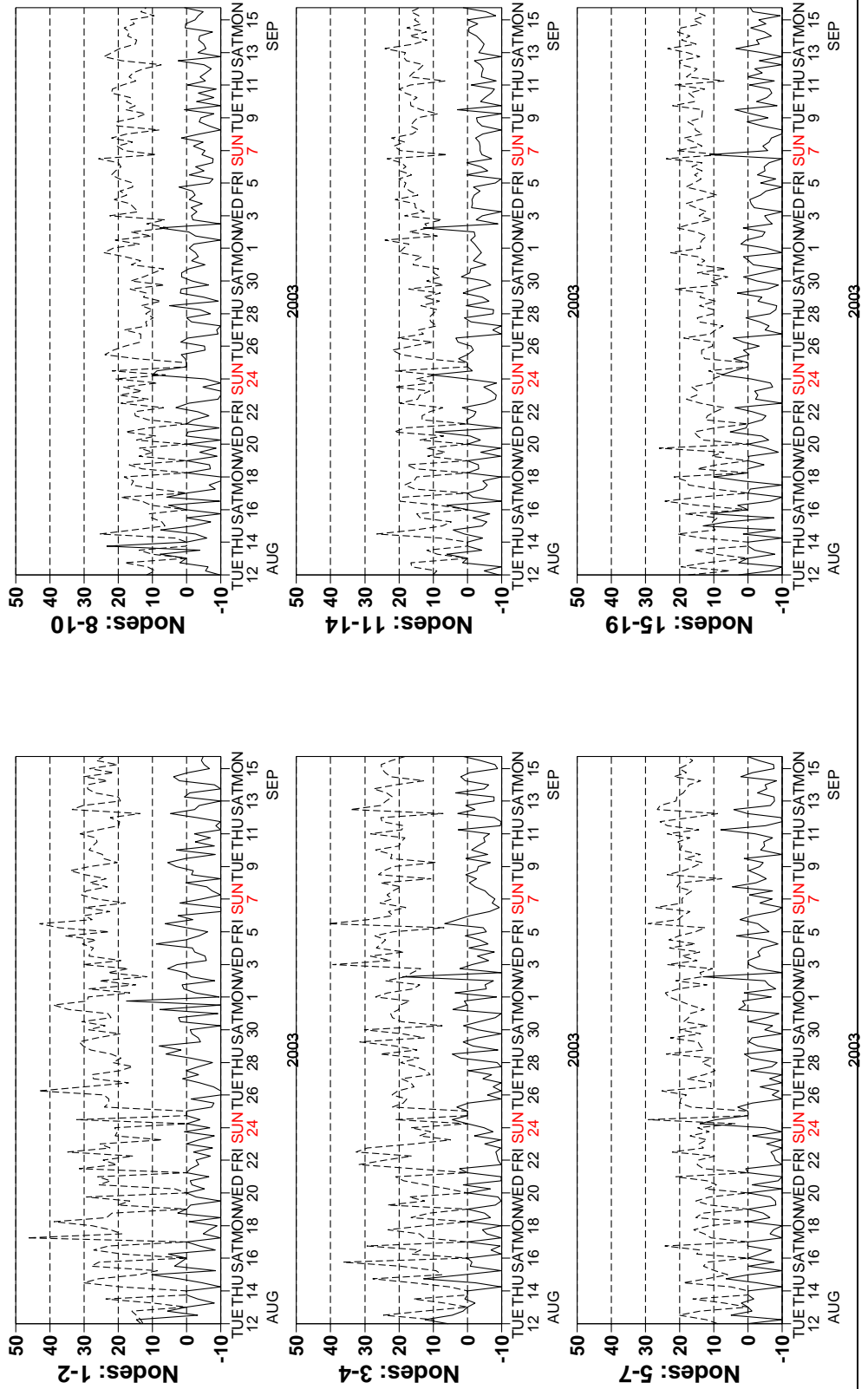


Figure 7

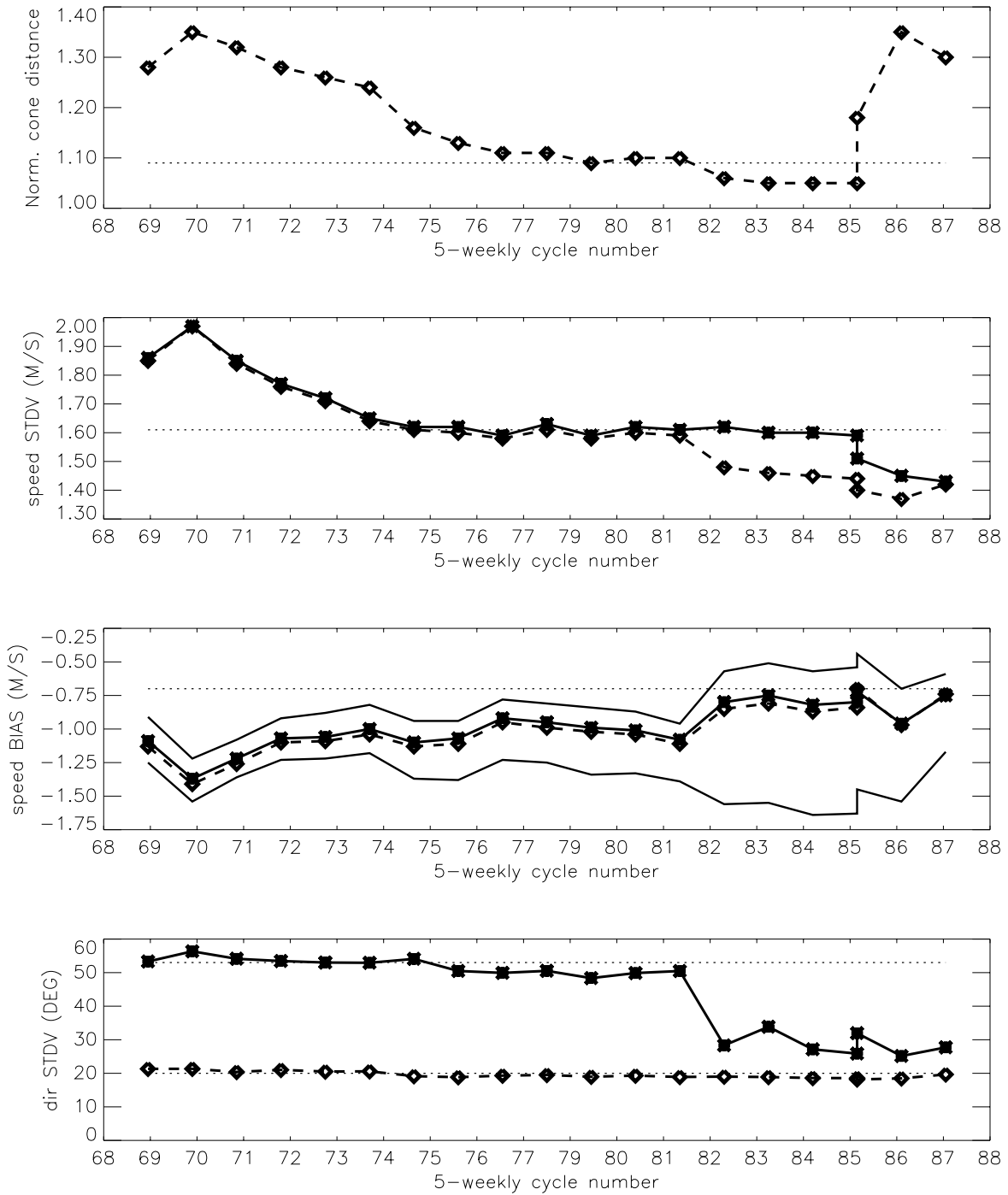


Figure 8

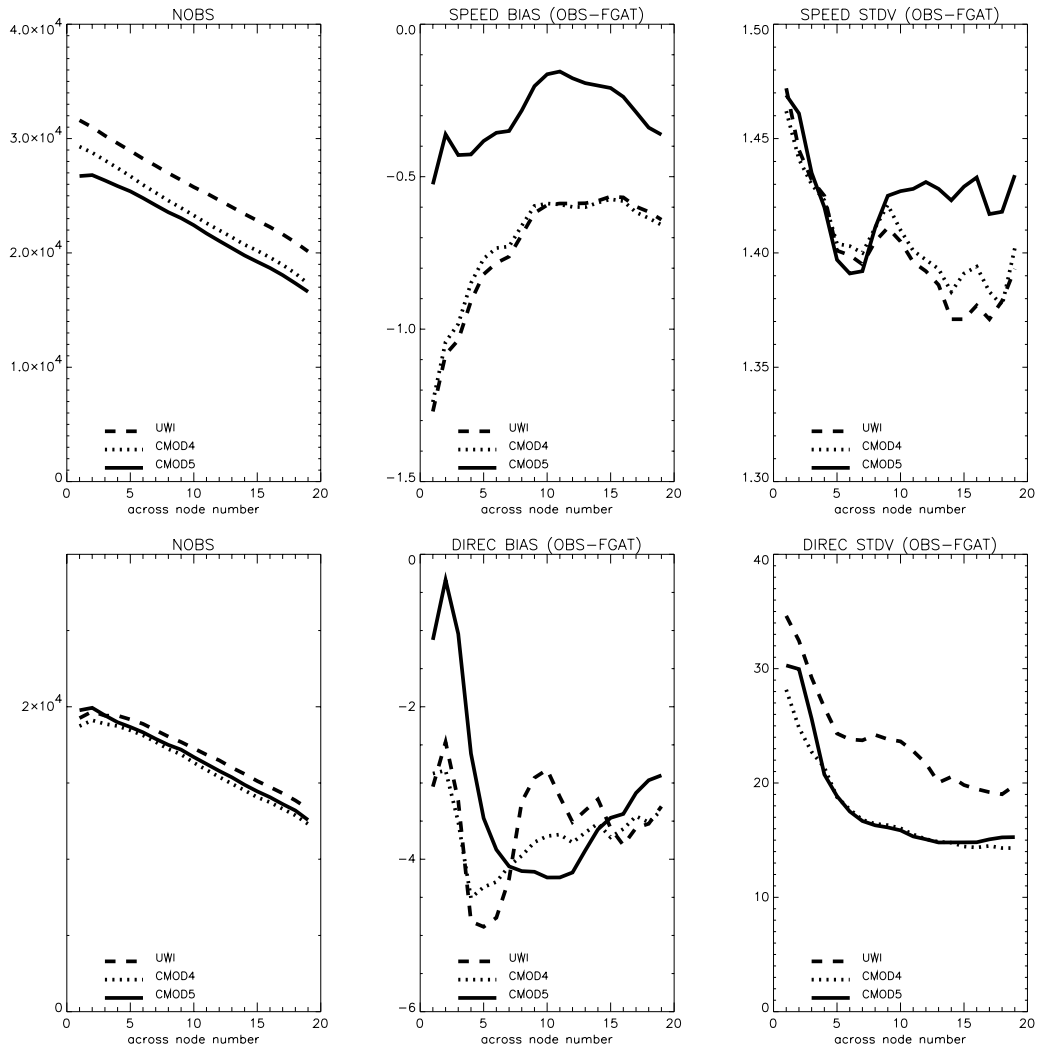


Figure 9

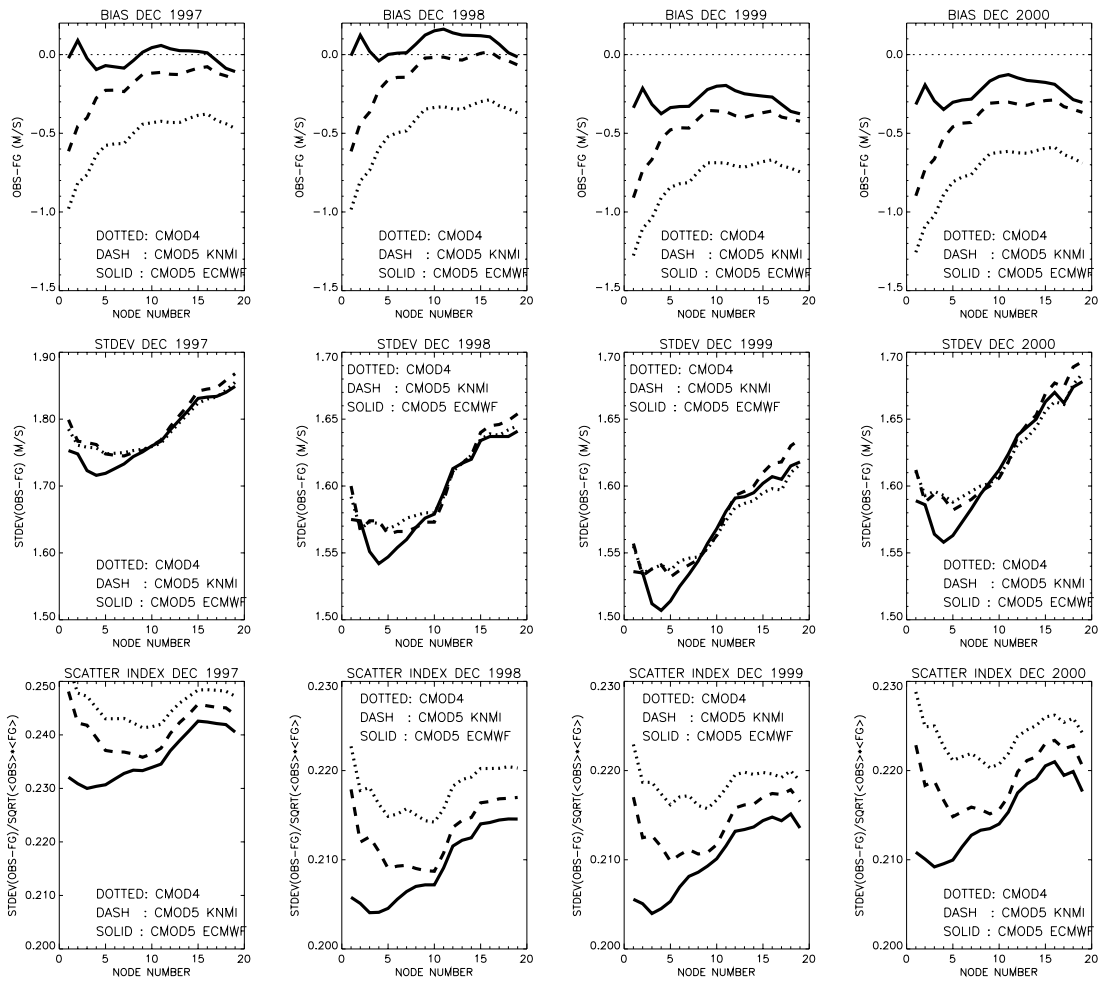
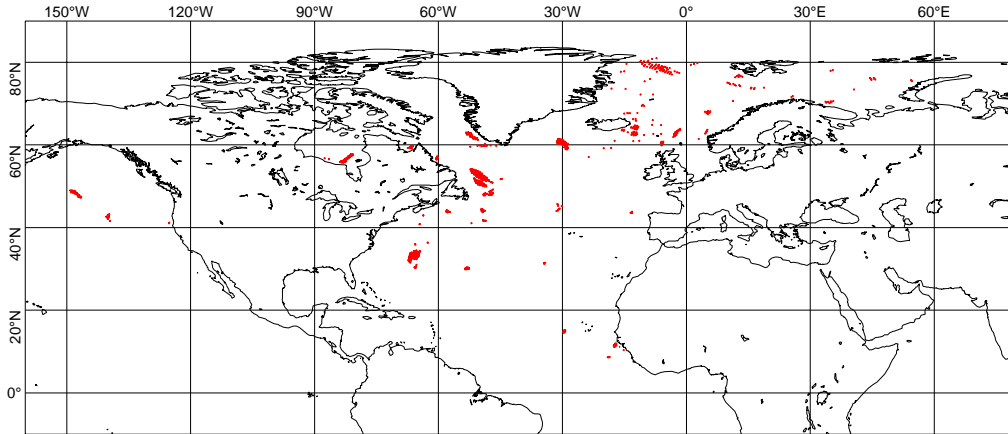


Figure 10

UWI winds more than 6 m/s weaker than FGAT  
cycle 87; 2003081200 to 2003091518



UWI winds (red) versus FGAT winds (blue)  
5 September 2003, 14:59 - 15:01 UTC

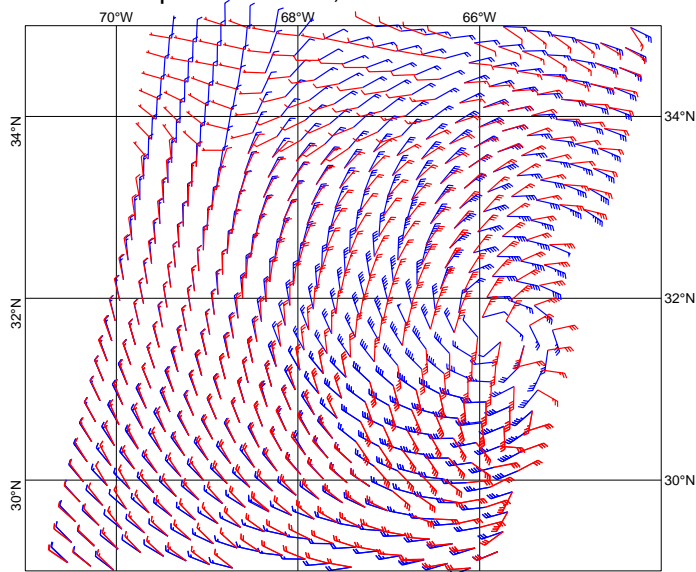


Figure 11

histogram of first guess 10 m winds versus uwi winds  
from 2003081200 to 2003091518  
= 491369, db contour levels, 5 db step, 1st level at 1.9 db  
 $m(y-x) = -0.75$   $sd(y-x) = 1.44$   $sdx = 3.12$   $sd_y = 2.90$   $pcxy = 0.943$

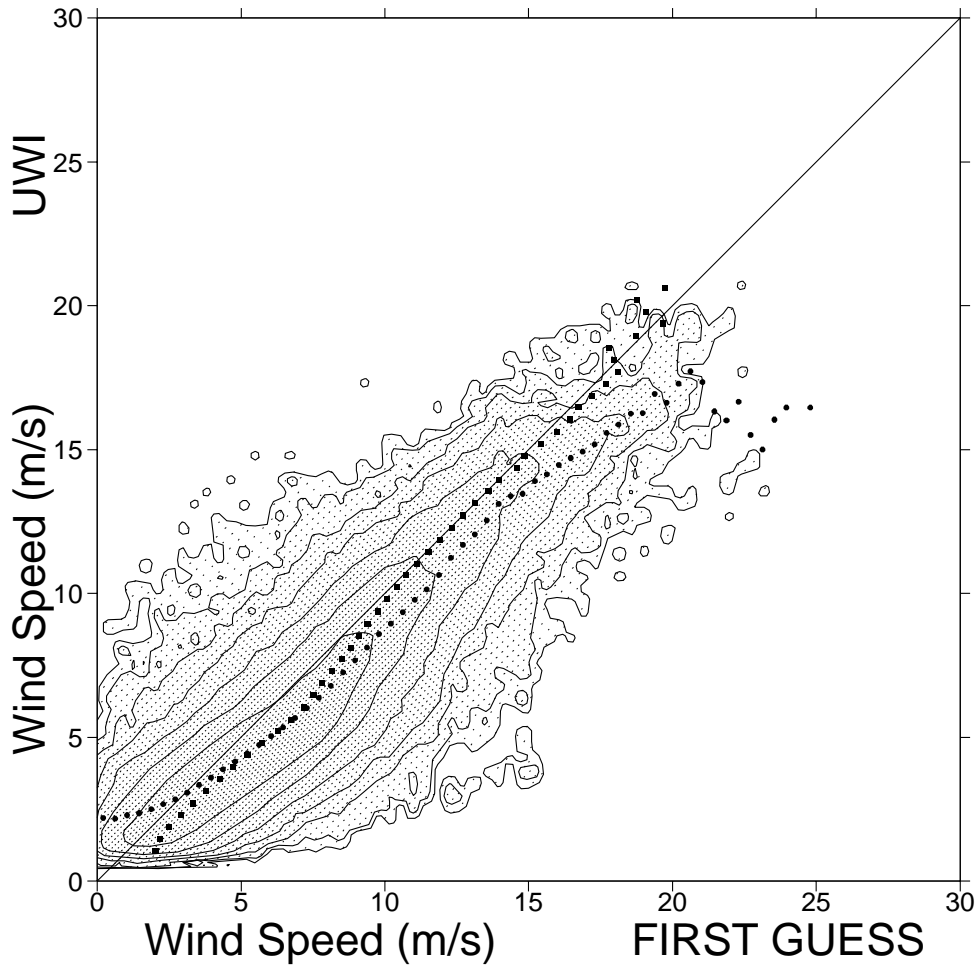


Figure 12

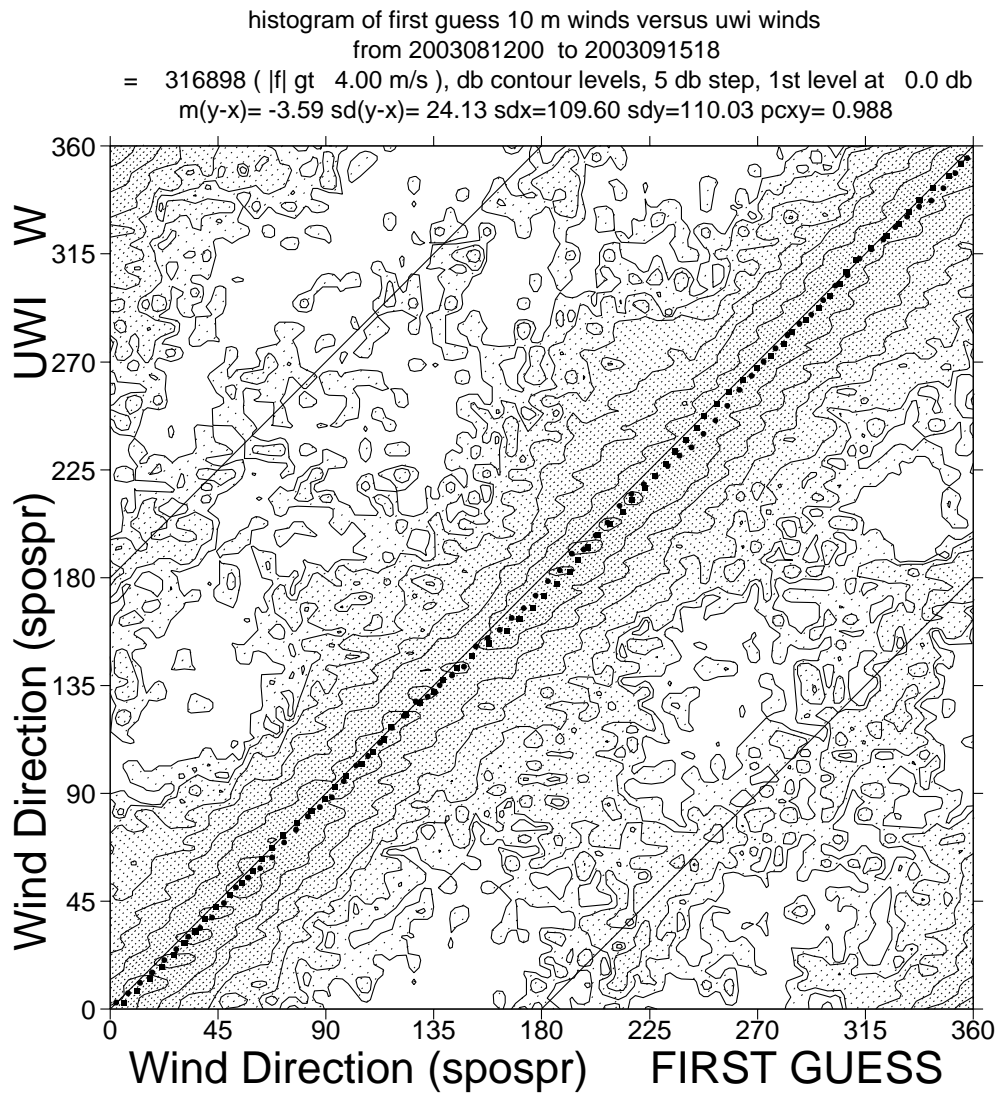


Figure 13

histogram of first guess 10 m winds versus CMOD4 winds  
from 2003081200 to 2003091518  
= 444271, db contour levels, 5 db step, 1st level at 1.5 db  
 $m(y-x) = -0.74$   $sd(y-x) = 1.44$   $sdx = 3.13$   $sd_y = 2.91$   $pcxy = 0.943$

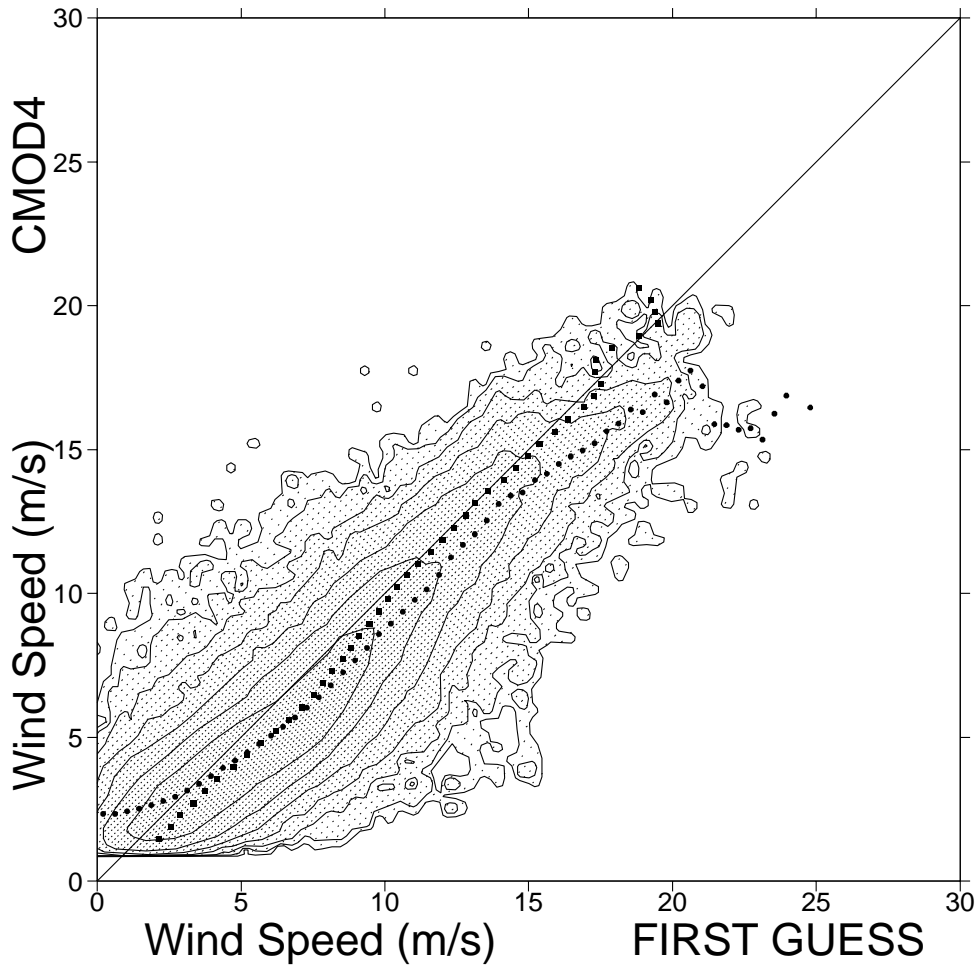


Figure 14

histogram of first guess 10 m winds versus CMOD5 winds  
from 2003081200 to 2003091518  
= 421967, db contour levels, 5 db step, 1st level at 1.3 db  
 $m(y-x) = -0.30$   $sd(y-x) = 1.45$   $sdx = 3.05$   $sd_y = 3.03$   $pcxy = 0.942$

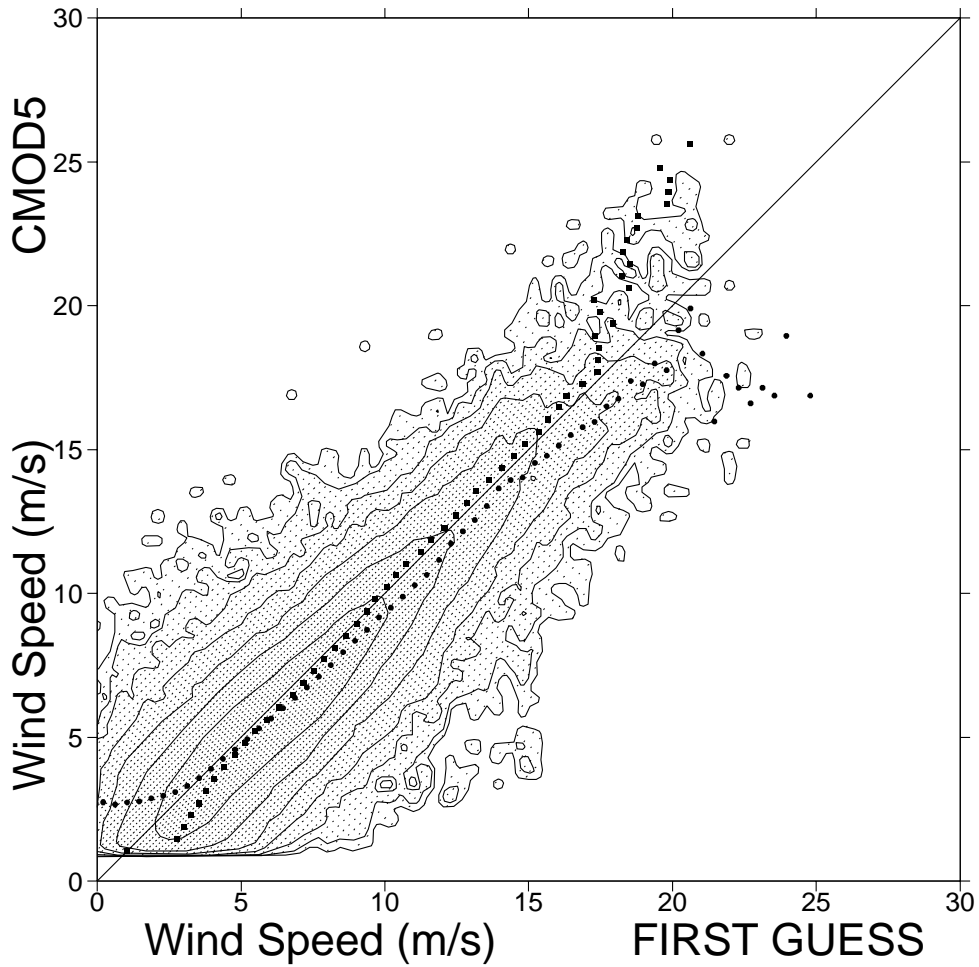


Figure 15